University of Baghdad
College of Engineering
JOURNAL OF ENGINEERING

Journal of Engineering

journal homepage: www.joe.uobaghdad.edu.iq

Volume 29 Number 11 November 2023

Verification and Parametric Analysis of Shear Behavior of Reinforced Concrete Beams using Non-linear Finite Element Analysis

Dunyazad Assi

Department of Civil Engineering, College of Engineering, University of Sulaimani, Sulaimani, Iraq.
Dunyazad607@gmail.com

ABSTRACT

Many researchers have tackled the shear behavior of Reinforced Concrete (RC) beams by using different kinds of strengthening in the shear regions and steel fibers. In the current paper, the effect of multiple parameters, such as using one percentage of Steel Fibers (SF) with and without stirrups, without stirrups and steel fibers, on the shear behavior of RC beams, has been studied and compared by using Finite Element analysis (FE). Three-dimensional (3D) models of (RC) beams are developed and analyzed using **ABAQUS** commercial software. The models were validated by comparing their results with the experimental test. The total number of beams that were modeled for validation purposes was four. Extensive parametric analysis has been carried out on another twelve beams to explore the influence of specific parameters, such as using different strengths of concrete, different flexural reinforcement bars, and laminate in the shear regions. It is concluded from the results that when a different compressive strength was assigned to RC beams, a decrease by 31 of beam ultimate strength was recorded when using C25 concrete strength. On the other hand, an improvement of 29% was observed by assigning concrete compressive strength C50. As well as another decrease of 18 and 26 kN was observed when GFRP was used with beams that had stirrups and beams that had both stirrups and SF. However, the beams recorded a higher number for ductility with using GFRP. In addition, using laminate with the beam that had both stirrups and SF was not beneficial; hence, the failure load was increased by only 3%, particularly with the beam that had both stirrups and SFs

Keywords: Finite element, FRP, RC Beams, Shear, Ductility.

*Corresponding author
Peer review under the responsibility of University of Baghdad.
https://doi.org/10.31026/j.eng.2023.11.11
This is an open access article under the CC BY 4 license (http://creativecommons.org/licenses/by/4.0/).
Article received: 25/01/2023
Article accepted: 27/04/2023
Article published: 01/11/2023

التحقق والتحليل البارامترى لسلوك القص لعوارض الخرسانة المسلحة باستخدام تحليل العناصر المحدودة غير الخطية

دنيازاد عاصي

قسم الهندسة المدنية، جامعة سليمانية، كليه الهندسة، سليمانية ، العراق
Dunyazad607@gmail.com

الخلاصة

تم تناول مسألة سلوك القص لعوارض الخرسانة المسلحة (RC) من قبل العديد من الباحثين من خلال محاولة استخدام أنواع مختلفة من التقوية في مناطق القص وكذلك باستخدام ألياف الحديد. في البحث الحالي تمت دراسة تأثير عدة عوامل ، مثل استخدام نسبة مئوية واحدة من الألياف الفولاذية (SF) مع وبدون اطواق ، بدون اطوق وبدون ألياف فولاذية ، على سلوك القص اعتاب RC ومقارنتها بواسطة باستخدام تحليل العناصر المحددة (FE). تم تطوير وتحليل النماذج ثلاثية الأبعاد (D3) للعتب (RC) باستخدام برنامج ABAQUS. تم التحقق من صحة النماذج من خلال مقارنة نتائجها مع الاختبار التجريبي ، وكان العدد الإجمالي للنماذج التي تم تحليلها لأغراض التحقق أربعة. تم إجراء تحليل حدودي شامل على اثني عشر اعتاب أخرى ، لاستكشاف تأثير عوامل محددة مثل استخدام قوى مختلفة للخرسانة ، وقضبان تقوية مختلفة ، واستخدام الصفائح في مناطق القص. يُستنتج من النتائج أنه عند تخصيص مقاومة انضغاط مختلفة لاعتاب RC ، تم ملاحظة انخفاض بمقدار 31 من المقاومة النهائية للعتب عند استخدام قوة الخرسانة C25. من ناحية أخرى ، لوحظ تحسن بنسبة 29٪ من خلال استخدام مقاومة انضغاط للخرسانة C50. بالإضافة إلى انخفاض آخر بمقدار 18 و 26 كيلو نيوتن لوحظ عندما استخدام GFRP مع اعتاب ذات اطواق واعتاب اخرى ذات اطواق و الياف حديد على التوالي. ومع ذلك ، سجلت النماذج عددًا أعلى من المرونة باستخدام GFRP. بالإضافة إلى ذلك ، لم يكن استخدام صفائح مع نموذج يحتوي على اطوق و الياف حديد مفيدًا ؛ وبالتالي ، تمت زيادة حمل الفشل بنسبة 3٪ فقط ، لا سيما مع النموذج الذي يحتوي على كلا من الاطواق و الياف الحديد.

الكلمات المفتاحية: العناصر المحددة ,الالياف الزجاجية , الياف كاربونية , اعتاب خرسانية مسلحة , قص

1. INTRODUCTION

Researchers have concentrated on material strength and performance due to the demand for multistory construction demand. Steel bars with high strength and good ductility replace traditional reinforcement in concrete structures, decreasing the total quantity of reinforcement and increasing reinforcement spacing, easing construction and maintaining the quality of concrete pours. Over the past few years, many studies have been conducted on various experiments on beams' shear and flexure behavior, including high-strength reinforcement and strengthening by FRP material **(Banibayat, 2011; Soltani et al., 2013; Said and Abbas, 2013; Darwin et al., 2016; Naqi et al., 2020; Said and Tu'ma, 2021; Khalaf et al., 2021; Abbood et al., 2021; Li et al., 2022)**. **(Jun et al., 2018)** studied the

effect of steel fibers with varied stirrup ratios on the shear behavior of RC beams with high-strength steel reinforcement. The findings of the tests indicate that the addition of steel fiber boosts the beams' ultimate load and their failure deformation and stiffness; however, the effect of steel fiber reduces when the stirrup ratios are increased. **(Hai et al., 2011)** conducted a model to evaluate the effect of steel fibers on the shear behavior of 27 beams without stirrups. The beams were tested by them and based on the experimental work of other researchers. The result shows that the proposed model can make pretty accurate predictions about the shear strength of steel FRC beams. The beams were tested with 334 MPa, 480 MPa, and 667 MPa yield stress stirrups. Results indicate that for a specific concrete strength, the shear capacity increases according to the yield strength of the stirrups.

According to **(Tiwari, 2019)**, the Grondal bridge in Stockholm, Sweden, had many cracks in its web of concrete hollow box girders when it was thoroughly checked in 2001, just two years after it opened. The bridges are made so that they meet Swedish guidelines. However, it turns out that the designs don't have enough shear reinforcement in their limited serviceability states. It was seen that the cracks kept getting bigger, and the number of cracks kept increasing, which is a problem for the structure's durability and ability to do its job. Thus, it becomes necessary to impose solutions for crack control, such as strengthening the shear region or including steel fibers, as it is well-known that steel fibers bridge cracks and prevent them from widening. (**Assi, 2011)**, furthermore, fibers contain microcracks and thus protect concrete from aggressive environmental attacks. In this regard, studies based on actual experiments have approved that a specific quantity of steel fibers added to the concrete ingredients significantly improves the shear and flexural strengths and elasticity of steel fiber-reinforced concrete (SFRC) flexural members **(Bencardinoa and Spadea, 2010; Luigi, 2017)**.

Based on **(Abbas, 2010)**, community FRP laminates are chosen over steel plates because of their superior tensile strength, high strength-weight ratio, and corrosion resistance and have become more popular as external reinforcement for the strengthening or rehabilitation of (RC) structures over the past two decades. **(Jawdhari and Harik, 2018),** FE models were utilized to simulate the failure modes seen in testing RC beams strengthened in flexure using CFRP rod panels. Compared to the experiments, the FE models were accurate regarding the ultimate load, load mid-span deflection history, and failure mechanism. Parametric research was performed by **(Arduini and Nanni, 1997)** to examine the impact of FRP on the strength and failure processes of repaired RC beams. The investigation aimed to investigate the effect of FRP factors such as stiffness, bond length, and adhesive stiffness when used as a repair material. The software does a nonlinear analysis and simulation of a beam. ANSYS.

After comparing the simulation findings with the experimental work of Zana and Serwan, the model is calibrated by considering the impact of openings on the behavior of RC beams in general and their shear strength in particular (2019). After the adjustment, the numerical results' load-displacement curve, crack pattern, and ultimate load agree closely with those from the experiments. However, most studies of (RC) structures exhibit enhancement with using FRP, according to **(Hsuan et al., 2004)** in the literature. It is commonly accepted that unidirectional fiber composites' in-plane shear stress-strain relations are highly nonlinear. The importance of accurately modeling FRP's nonlinear behavior cannot be overstated. From the experimental study **(Masmoudi et al., 2012)**, GFRP bars have a weaker elasticity modulus, with more deflection for equal loads and spans.

This work uses the finite element program ABAQUS to perform failure analysis of rectangular (RC) beams with multiple variables, including strengthening with FRP. In the modeling process, four beams are tackled to have the same material properties and geometry as beams tested by previous researchers for validation purposes; those beams were reinforced with high-strength steel bars and different stirrup ratios with and without steel fibers. In addition, twelve other beams were molded for a parametric study; these beams had different concrete compressive strengths and reinforcement materials and were reinforced with FPR in the shear region. This work examines the global nonlinear behavior of rectangular reinforced concrete beams subjected to two-point loads, dispersed loads, and FRP laminate strengthening.

2. FINITE ELEMENT MODEL

In this section, 3D finite element (FE) models are developed using the commercial software ABAQUS to study the behavior of reinforced concrete beams subjected to a two-point load. The geometric description of test beams extracted from the tests of **(Jun et al., 2018)** is shown in **Fig. 1 (a, b, c)**. All beams have identical dimensions of 150 mm width, 300 mm depth, and 2100 mm span center to center. Beams that S0000 and S0010 denoted have no shear reinforcement and are designed with only bottom reinforcement of 2ϕ25 mm steel bars.

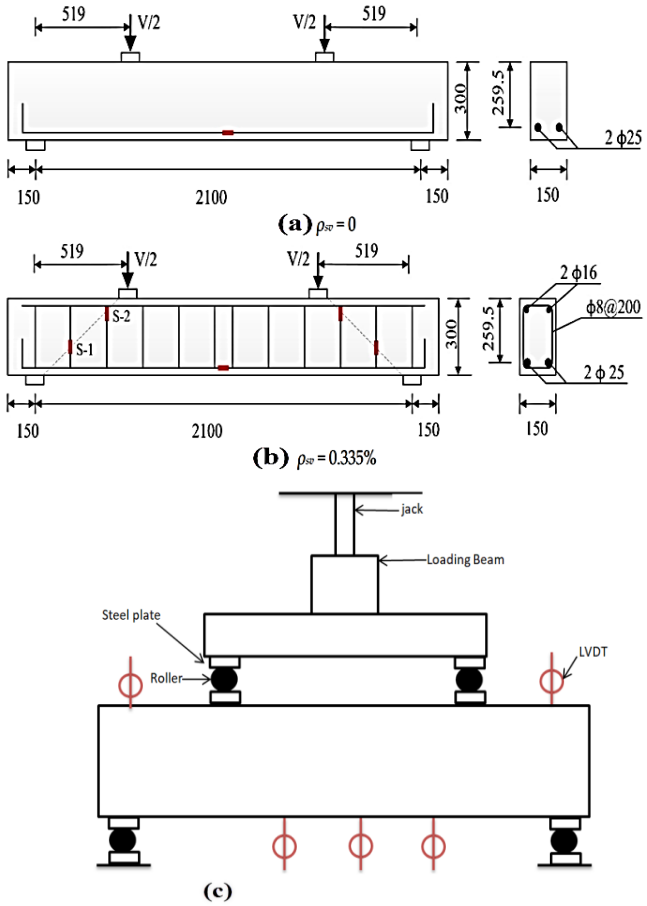

Figure 1. Schematic diagram of adopted particulars of experimental beams (all dimensions in mm). a) Specimens without stirrups, b) Specimens with 0.335% stirrup ratio, c) Diagram of experimental beam loading.

It is worth mentioning that beams S0000 and S0010 have 0.0% and 1.0% steel fibers, respectively. While, beams denoted by S0300 and S0310 were reinforced with 2ϕ25 mm bottom bars, 2ϕ16 mm top bars, and ϕ8@200 mm for shear reinforcement. Also, these two beams have the same formation percentages of steel fibers. Both material and geometrical non-linearity are considered in the finite element analysis. The material properties are given in **Tables 1 and 2**, as stated by the researchers. While the remaining data was obtained using the ACI code 318 **(Bloem and Delevante, 1970).** Furthermore, a parametric study was performed on another twelve beams with the same material properties of beams **(Tarek et al., 2013; Chellapandian et al., 2017; Jun et al., 2018).**

Table 1. Major details of the experimental beams from (**June et al., 2018)**

Beam ID	Stirrups	ρ sv (%)	Vf (%)	fc (MPa)	ft (MPa)	Es (MPa)	Vu,exp (kN)
S0000	-	0	0	33.03	3.72	23,713	185
S0010	-	0	1.0	36.08	5.33	25,968	276
S0300	ϕ8@200	0.335	0	33.03	3.72	23,713	347.61
S0310	ϕ8@200	0.335	1.0	36.08	5.33	25,968	378.02

Table 2. Major properties of high strength reinforcement

Diameter (mm)	Yield Strength (MPa)	Ultimate Tensile Strength (MPa)	Percent Elongation (%)
8	641.9	848.4	9.0
16	585.5	740.8	14.4
25	567.8	735.5	14.6

The steel bars were simulated by adopting the classical metal plasticity available in ABAQUS; an elastic-perfect plastic relation was assigned regarding the stress-strain curve shown in **Fig. 2a**. However, in addition to the reinforced steel bars used in the four modeled validation beams, two other different reinforcement bars are used in the parametric study, having the same diameter to those used by (Jun et al., 2018) they were glass and carbon fiber polymer reinforcement (GFPR and CFPR). Three-dimensional, two-node truss elements with (6) degrees of freedom (DOF) at each node and decreased integration were used to describe the bar and stirrup geometry (T3D2R). FRP is a brittle material that shows a sudden failure after yielding strength. As a result, the behavior of FRP bars was simulated, as shown in Fig. 2b. Because it can model concrete in both plane and reinforced forms, the concrete damage plasticity (CDP) model was used to simulate the material. The CDP model required defining three main sections: plasticity parameters, compressive behavior, and tensile behavior. The plasticity parameters were calibrated so that the concrete behavior matched the experimental response **(Chang et al., 2006**; **Kodur and Agrawal, 2016; Sonnenschein et al., 2016; Abraham et al., 2016).** However, the compressive and tensile behavior was entered depending on the available experimental data and by adopting (**Saenz, 1964)** for normal concrete, while the stress-strain curve adopted (**Chalioris, 2018)** was used to simulate the steel fibers.

On the other hand, (**Hordijk, 1992)** was adopted regarding the tensile behavior of concrete. A mesh size of 25 was chosen based on a sensitivity study; this delivers stable results with minimal processing overhead.) The boundary condition was assigned as

indicated in the experimental test (support). The load was applied through loading plates tied to the top concrete surface, as shown in Fig. 3a. Apart from using different concrete strengths and bar types in this parametric study. The beams were strengthened in the shear regions with CFRP laminates, as shown in **Figs. 3 a, b, and c** above-mentioned. The 3D solid shell with dimensions 150×300×519 mm and 0.167 mm thick, as shown in **Fig. 3b,** is used to model CFRP laminate.

The physical and mechanical properties of the laminate used in the simulation are taken from (**Chellapandian, 2017),** in which density is 1820 kg/m^3, E-value is 81.9 GPa, and tensile strength is 1188 MPa.

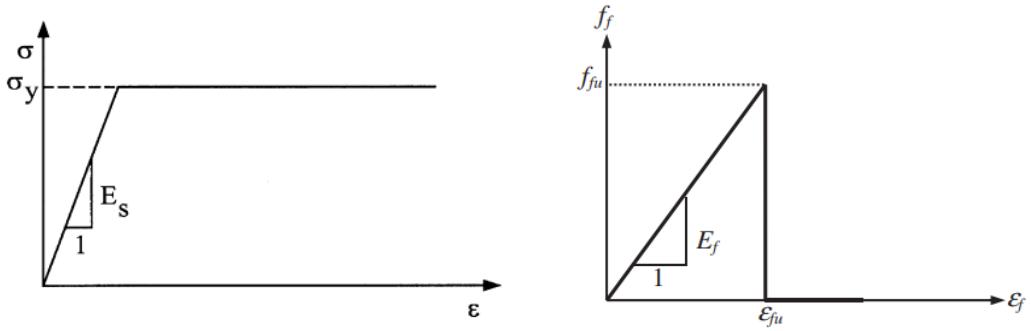

(a) Steel bars **(b) GFRP bars**

Figure 2. Stress-strain curve simulation for Steel and GFRP bars from ABAQUS 19 and (**Hsuan, 2004)**, respectively

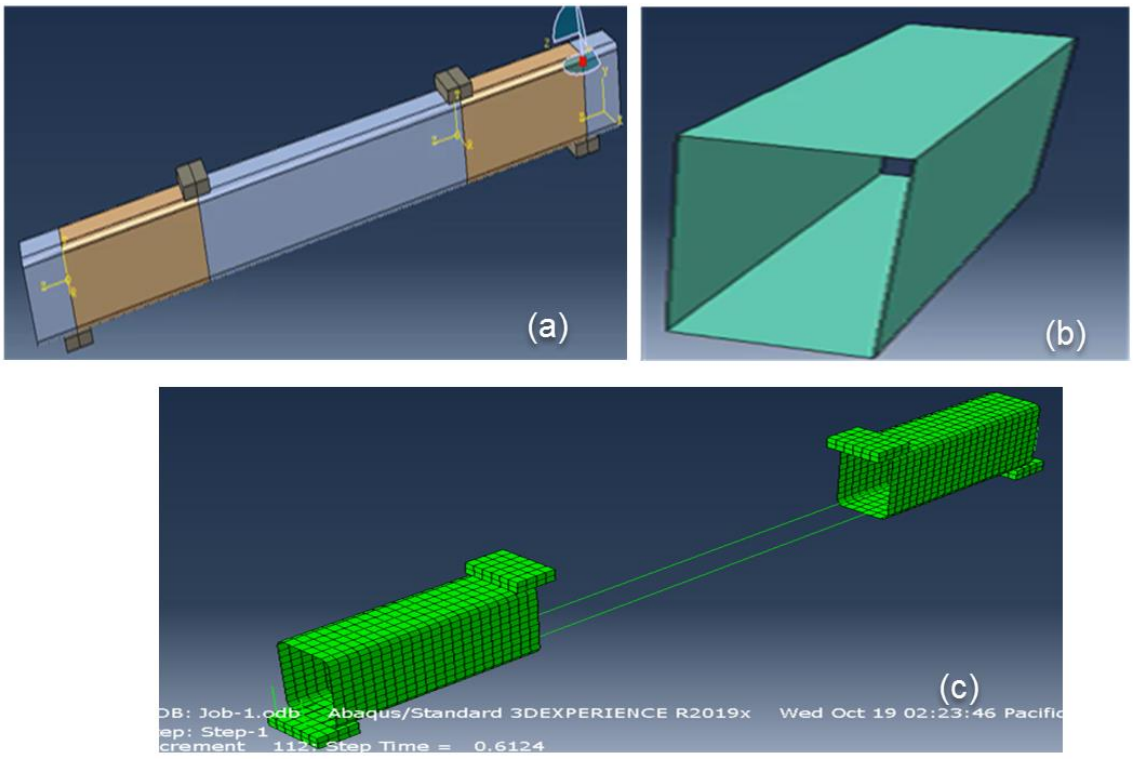

Figure 3. a) Simulated beam with laminate layers in both ends of the shear region, b) and c) Simulated Laminate layer

3. VERIFICATION OF THE PROPOSED MODELS

The validated FE models of beams are verified by previous experimental results obtained from the tests of **(Jun et al., 2018),** from which the reinforcement details and the geometric descriptions of the modeled beams are taken and provided in **Tables 1 and 2** and **Figs. 1a, b, and c**. In these tests, the dimensions of the test beams were 2100 mm in length, 150 mm in width, and 300 mm in height, and the shear span ratio was 2. The longitudinal bars consisted of two 25-mm-diameter steel bars; the reinforcing ratio of longitudinal bars was 2.52 percent, and the concrete cover depths of all beams were 20 millimeters. This study considers two key variables: stirrup ratio (sv = 0) and fiber volume fraction (Vf = 0% and 1%). Beams with 0% or 0.335% stirrup ratios had (Vf = 0%, 1%) fiber volume fractions. **Fig. 4** indicates the comparison of load-mid-span displacement curves, while **Table 3** compares ultimate loads for each test between the FEA and test results **(Jun et al., 2018)**. **Table 3** shows that the largest discrepancy between FEA and test data for the ultimate strength of these beams is 2.2%. In addition, **Fig. 4** demonstrates that the FEA curves correspond well with the experimental curves. Furthermore, as shown in **Fig. 5**, the failure modes gleaned from FEA results agree with those gleaned from the destructive testing of the beams. Therefore, it can be concluded that the FE model accurately predicts the behavior of RC beams that include steel fibers with and without stirrups and beams with and without steel fibers, in addition to beams with neither steel fibers nor stirrups.

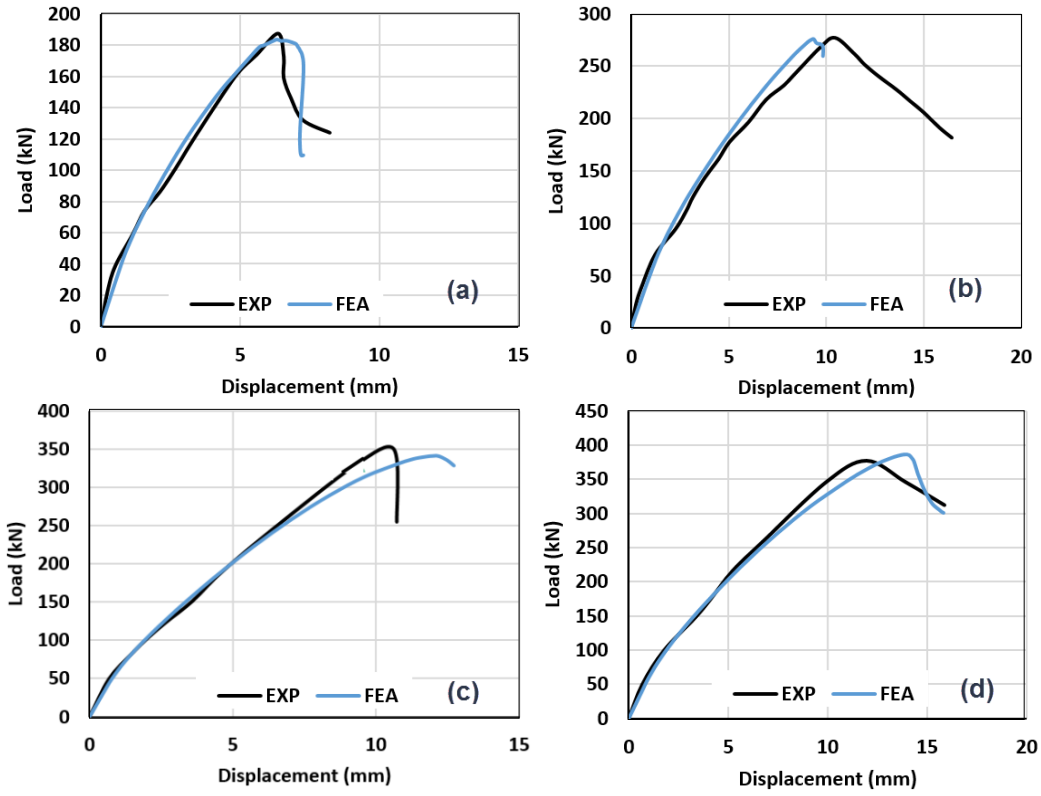

Figure 4. Load displacement curves for different beams (a) S0000, (b) S0010, (c) S0300, and (d) S0310, respectively **(Jun et al., 2018)**

Table 3. Comparison of shear resistance obtained from Experimental Test of **(Jun et al., 2018)** and the FEA.

Designation	ρ_{sv} %	% SF	Vtest (KN)	VFEA (KN)	VFEA/Vtest
S0000	0	0	185	183	0.989189
S0010	0	1	276	270	0.978261
S0300	0.335	0	347.61	342	0.983861
S0310	0.335	1	378.02	385	1.018465

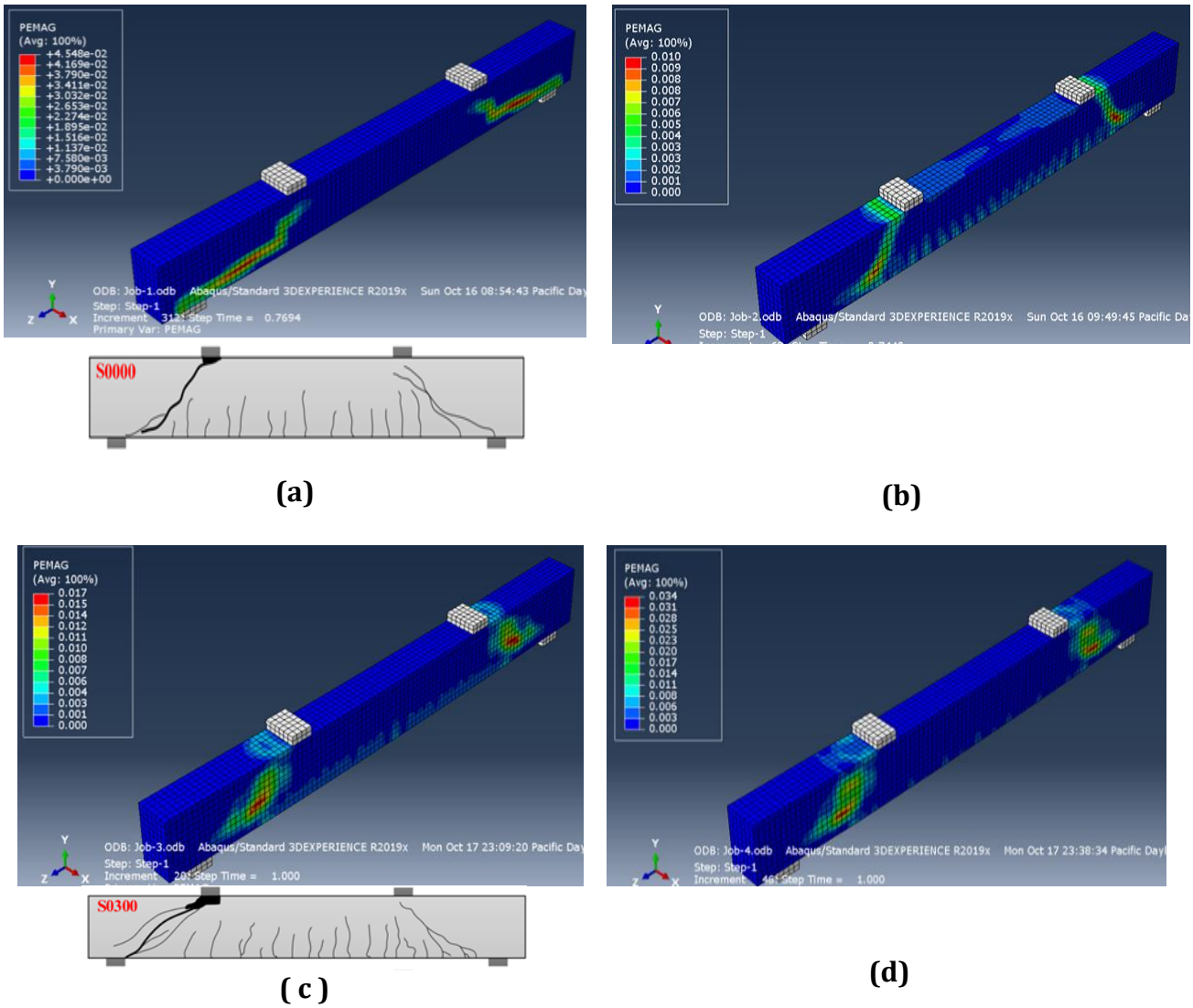

Figure 5. Comparison between failure modes obtained from FEA and EXP from **(June et al., 2018)** (a) S0000, (b) S0010, (c) S0300, and (d) S0310.

4. PARAMETRIC STUDY

The (FEA) of the modeled beam specimens used in this parametric study focused on solving problems of shear failure of RC beams on a zone of variables larger than those covered by previous researchers. These dependent variables in this study are compressive strengths, steel ratio in the shear region, percentage of steel fibers, and different types of flexural reinforcement bars made of glass and carbon fiber reinforced polymer (GFRP and

CFRP). Hence, the modeled beams in this parametric study are sorted into five groups. Group A consists of four beams: one without stirrups and SF; one without stirrups but with 1% SF; one with 0.335% stirrups but without SF; and one with 0.335% stirrups and 1% SF. The second group is the same as Group A; however, the only difference is in the concrete's compressive strength, which is 35. In Group C, the beams are reinforced with bars with a 743 MPa yield strength (fy), an E-value of 40 GPa, and a 1900 kg/m^3 density. This group has a beam with 0.335% stirrups without SF and another with 1% SF. The fourth group is Group D. The difference between Group C and Group D is in the type of bar reinforcement used; hence, in Group D, the reinforcement bars were made of CFRP rather than GFRP, as in Group C. The properties of such kinds of bars are taken from **(Chellapandian, 2017)**, in which the Poisson's ratio is 0.3, and the elastic modulus is 89.4 GPa and 56 GPa for CFRP and GFRP bars, respectively. The tensile strengths of CFRP and GFRP bars were taken as 1157 and 1395 MPa, respectively. The last group, Group E, consisted of beams with the same variables considered as the beams in Group B. However, the beams in this group were covered and bonded to a layer of CFRP laminate in the shear regions. The properties of the laminate layers are mentioned in the previous item in this paper. The properties of the proposed beams are given in **Table 4**.

It is important to remember that the first two numbers of the beam ID reflect the concrete grade, the first letter represents the shear, the next two digits represent the stirrup ratio, and the last two digits represent the fiber volume percent. The bar type is indicated by the previous letter C or G, while L indicates the lam.

5. RESULTS OF THE PARAMETRIC STUDY

The load-displacement results and failure modes for the different parameters per Finite Element analysis**.**

5.1. Effect of Decreasing the Concrete Grade of Failure Load.

Comparing the results of load-displacement curves shown in Fig. 6a for the beams C25 and C33, it's clear that beam C25 failed at a load of 155 kN at 5.5 mm, while the failure load of beam C33 is 180 kN at the same displacement value. This means that the beam with higher compressive strength has a load-bearing capacity of 16% more than that of the beam of lower compressive strength. However, 1% steel fiber **(Fig. 6b)** increased the failure load for beams C25 and C33 cases. The failure load of beam C25 reached 240 kN at a deflection of 9.5 mm, and the value of failure load in the case of beam C33 reached 270 kN at the same deflection value, i.e., the difference in the failure load value between C25 and C33 is 9.5%.

Table 4. The details of the modeled beams

Beam designation	Description	Type of bars	fy (MPa)	Stirrups ρ_{sv} %	Steel Fibers %
25S0000&33S0000	(Group A) fc =25 (MPa) & (Group B) fc =33 (MPa)				
25S0010&33S0010 25S0300&33S0300	Beam without stirrups without steel fibers	Steel	576.8	0	0
25S0310&33S0310	Beam without stirrups with steel fibers 1%	Steel	576.8	0	1
	Beam with stirrups without steel fibers.	Steel	576.8	0.335	0
	Beam with stirrups with steel fibers 1%.	Steel	576.8	0.335	1
33S0300G 33S0310G	Group C fc = 33 GFRP-Beam with stirrups without steel fibers.	GFRP		0.335	0
	GFRP-Beam with stirrups with steel fibers 1%.	GFRP		0.335	1
33S0300G 33S0310G	(Group D) fc =33 (MPa) CFRP-Beam with stirrups without steel fibers.	CFRP		0.335	0
	CFRP-Beam with stirrups with steel fibers 1%.	CFRP		0.335	1
33S0000L 33S0010L	(Group E) fc =33 (MPa) LAM-CFRP-Beam without stirrups without steel fibers.	CFRP		0	0
33S0300L 33S0310L	LAM-CFRP-Beam without stirrups with steel fibers 1%.	CFRP		0	1
	LAM-CFRP-Beam with stirrups without steel fibers.	CFRP		0.335	0
	LAM-CFRP-Beam with stirrups with steel fibers 1%.	CFRP		0.335	1

Figs. 6a and b, the beams had no shear reinforcement. Whereas beams in **Fig. 6c** that had shear reinforcement but without steel fibers reached a higher value of load in both cases, C25 and C33. However, C33 failed at a higher load value of 345 kN and deflection of 12 mm than C25, which fell at 250 kN and deflection of 10 mm. Insignificant variation in load-carrying capacity at low-grade concrete is noted when the beam had no stirrups, but the difference in failure load appeared when implemented strips were implemented. The beams in **Fig. 6d** have the same constituents as beams in **Fig. 5c** with one exception: beams in **Fig. 5d** include steel fibers beside stirrups; hence, it is obvious from the drawing curves that, besides the increase in failure load for beam C33 that reached 390 kN, the inclusion of steel fibers added more ductility, so the beam reached a deflection of 15 mm.

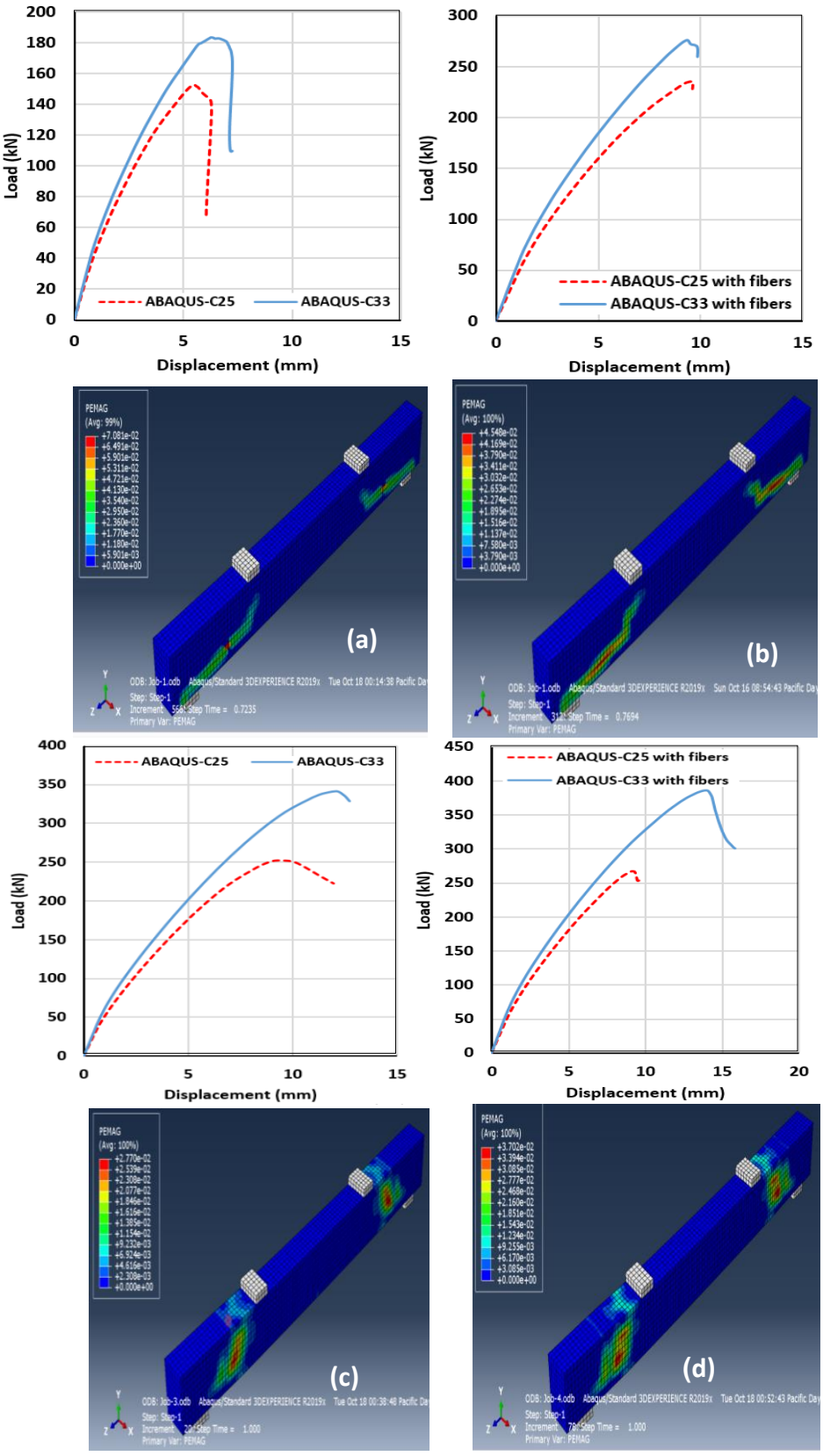

Figure 6. Load displacement curves for the known variables of beams with the mode of failure for the beams C25, a) S0000, b) S0010, c) 0.0300, d) S0310

The increase in ductility due to the inclusion of steel fibers is very obvious in **Fig. 6.b**, so the failure mode transferred from a pure shear failure in **Fig. 6a** to a ductile bending failure with small cracks. However, the presence of fibers in the beams in **Figs. 6c and 6d** that had shear reinforcement were not very effective in the failure mode, but the pure shear failure was disturbed due to stirrups.

5.2 Effect of Increasing Concrete Grade on the Failure Load

As shown in Figs, another load-bearing increase was observed when the concrete's compressive strength was increased**. Figs. 7 a, b, c, and d,** it is obvious that the beam with compressive strength 50 MPa (C50) has a greater load failure value than the beam with C33. When the beam had neither stirrups nor steel fibers, the failure load in beam C50 reached 280 kN at a deflection of 7.5 mm. While beam C33, as previously mentioned, reached 180 kN, beam C50 failed at a load greater than C33 by 56%.

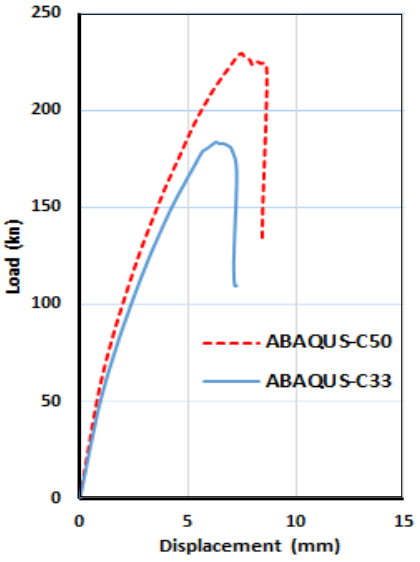

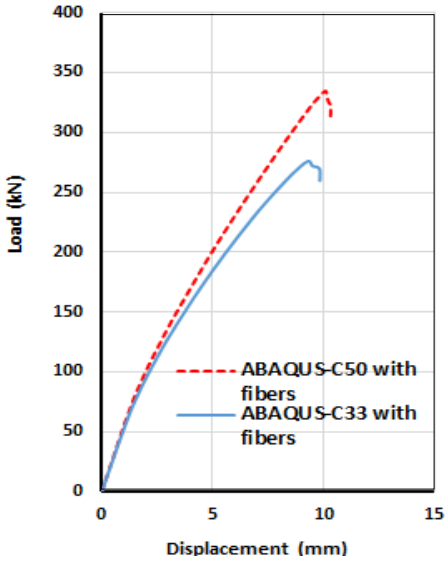

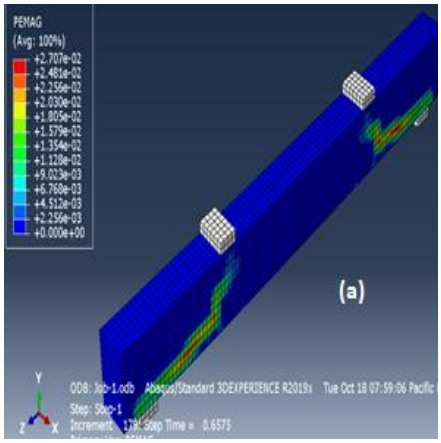

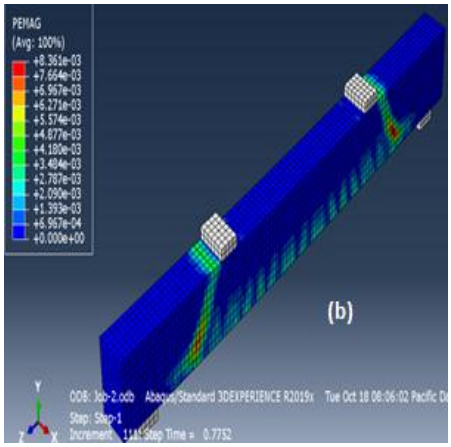

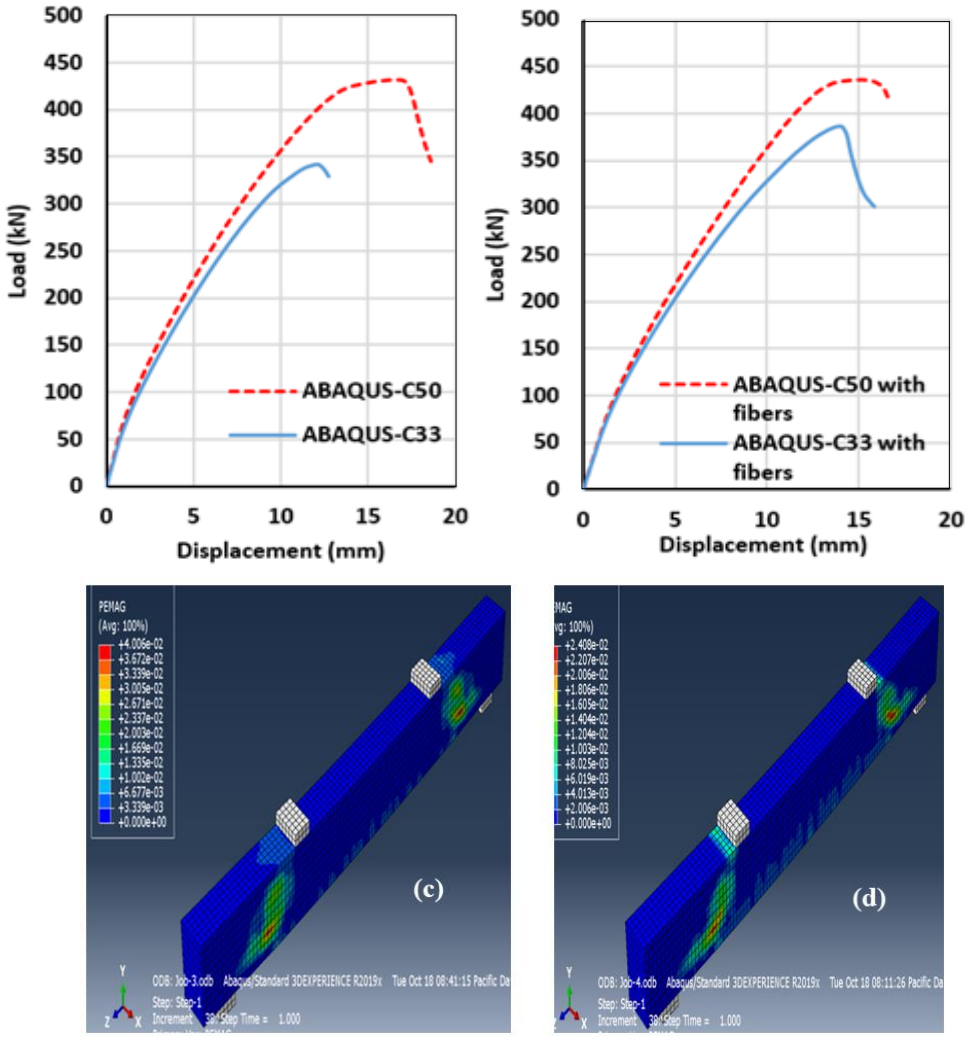

Figure 7. Load displacement curves for the known variables of beams with the mode of failure for beams C50 and C33. a) S0000, b) S0010, c) S0300, d) S0310

However, at the inclusion of 1% SF, the mode of failure tried to be more ductile, as shown in **Fig. 7b,** so the deflection reached 10 mm and a load value 340 kN higher than the load of beam C33 and higher than the load value of beam S0000, in which SF is 0%. So, the load continues to increase when the beam is reinforced in the shear region with stirrups, as shown in **Fig. 7(c, d)** and given in **Table 5**. In addition to the increase in load, the ductility increases in the case of the beams in the last two mentioned figures.

5.3 Effect of using GFRP Reinforcement Bars rather than Steel Bars

Another comparison between failure loads appeared in **Fig. 8 (a and b)**. The difference between these two beams and the other considered beams is the type of reinforcement bars used. Here, the bars used are GFRP bars with more ductility than normal high steel bars.

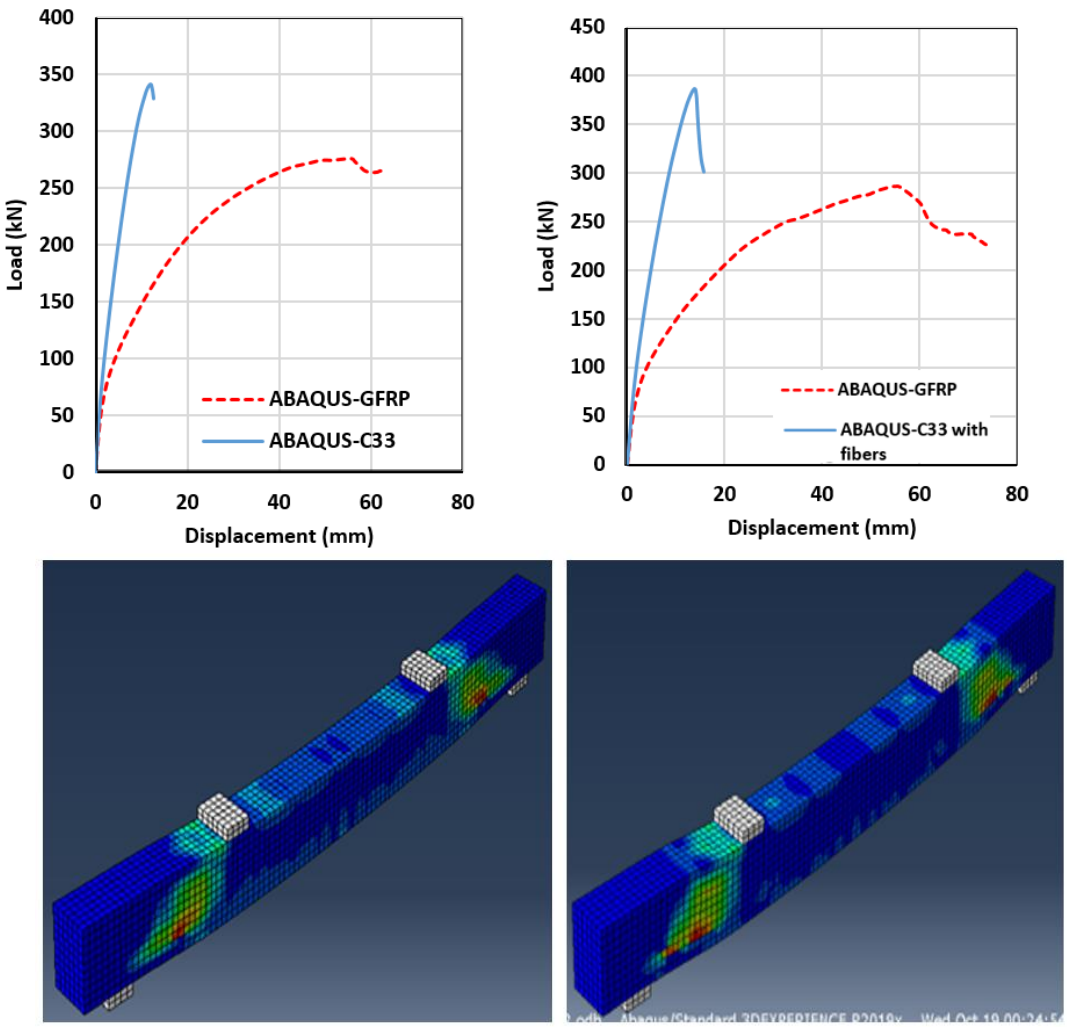

a) S0300 **b)**S0310

Figure 8. Load displacement curves for the known variables of beams with the mode of failure for the GFRP beams

This is clear from **Figs. 8 a and b**. Hence, the deflections in these two figures reached 60. The beam contained no SF as in **Fig. 8a** and 70 mm when the beam included 1% SF. However, the beams failed at a lower load value than the failure loads of the beam with normal high-strength steel bars. The failure loads are recorded in **Table 5**.

5.4 Effect of using CFRP Reinforcement Bars rather than Steel Bars

Regarding the effect of CFRP, as shown in **Figs. 9 (a and b),** they failed around the same load value of the beams C33; the difference is in the deflection value. The beams reinforced with CFRP bars that have a deflection of 30mm at failure load are more ductile than the beams C33.

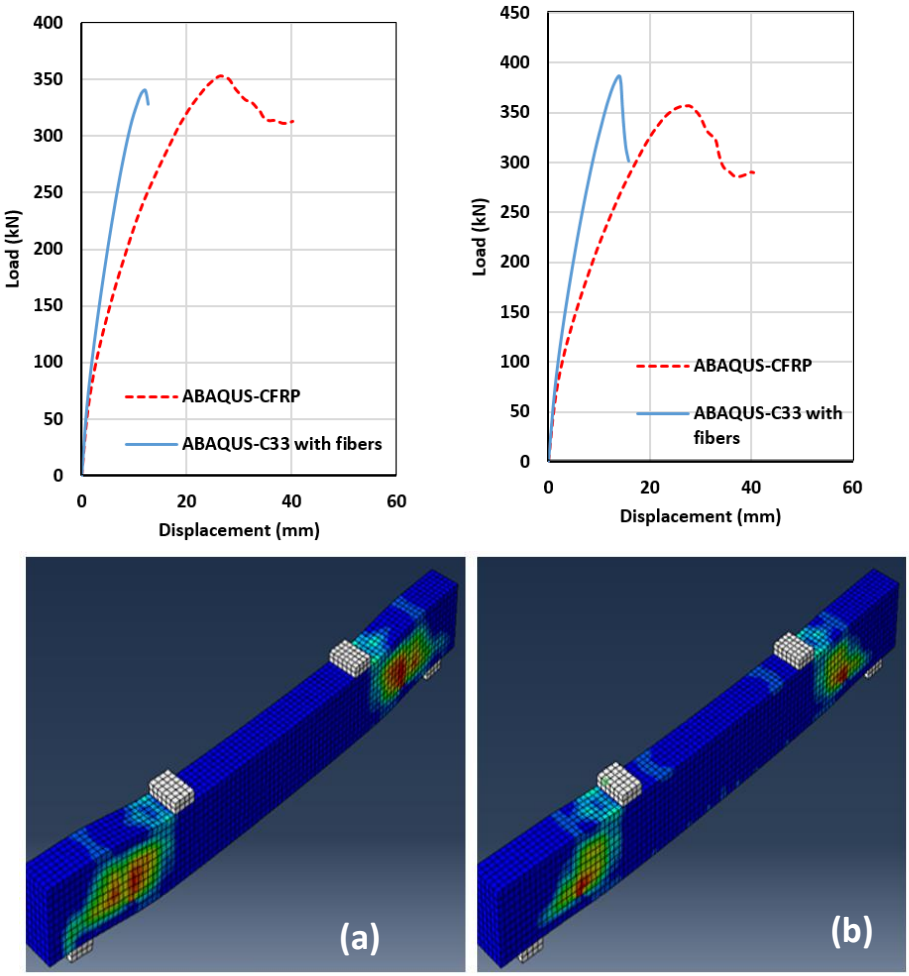

Figure 9. Load displacement curves for the known variables of beams with the mode of failure for the CFRP beams, **a)** S0300, **b)** S0310

Table 5. Illustration of failure load for modeled beams

	Stirrup %	SF %	Load (kN)						%				
			C33	C25	C50	GFRP	CFRP	Lam	C25 /C33	C50 /C33	GFRP /C33	CFRP /C33	Lam /C33
S0000	0	0	183	153	229			200	-16	25			4
S0010	0	1	276	235	334			294	-15	21			7
S0300	0.335	0	336	252	432	276	353	377	-25	29	-18	5	12
S0310	0.335	1	387	267	435	286	357	397	-31	12	-26	-2	3

5.5 Effect of using CFRP Laminate

CFRP laminates are carbon-based composite materials that attach externally to concrete beams. **Fig. 10** shows the effect of CFRP laminate, and **Table 5**. summarize the results. It can be noticed that these high strength materials improve the behavior of beams by increasing the failure load.

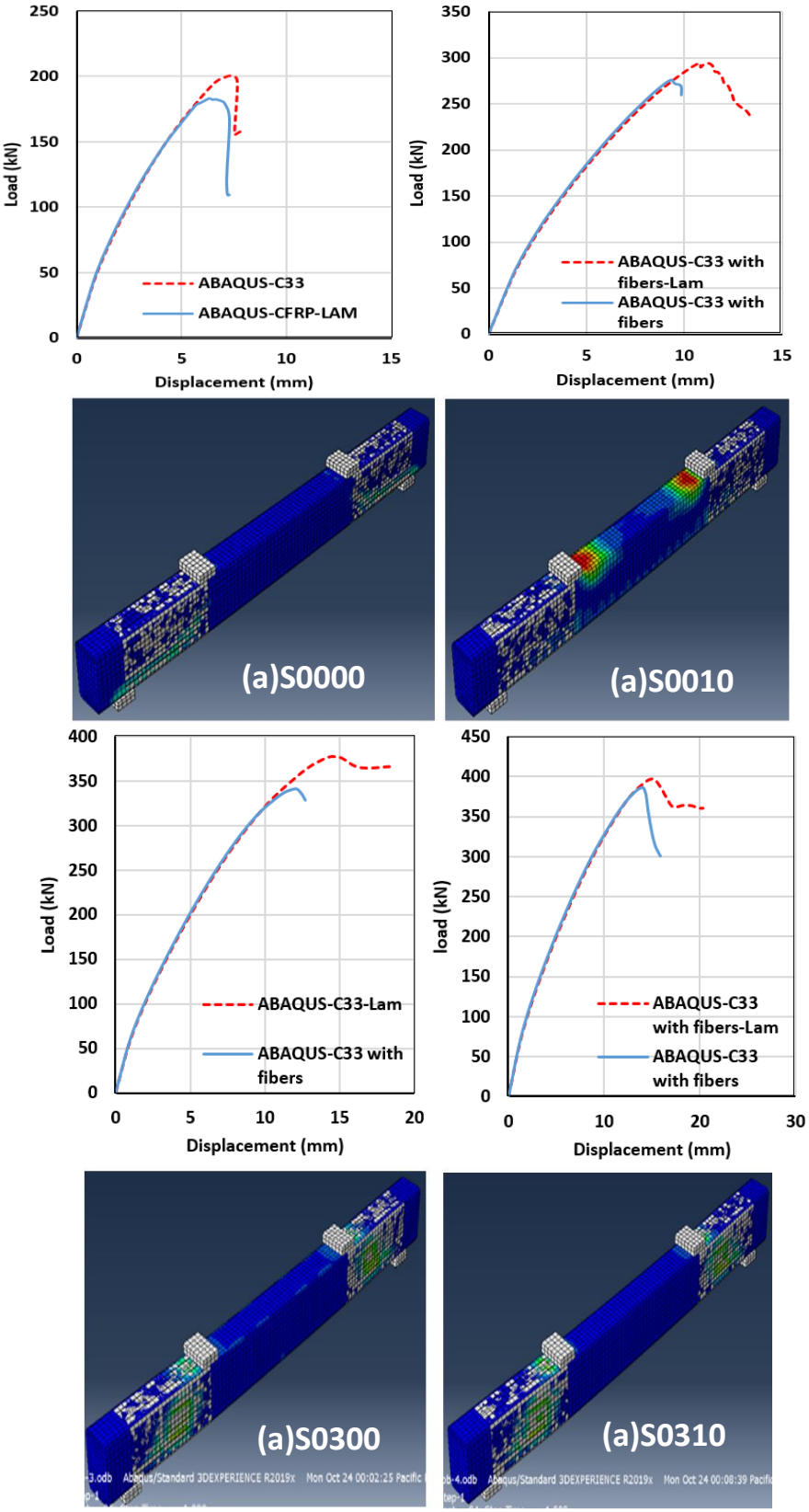

Figure 10. Load displacement curves for the known variables of beams with the mode of failure for the Laminated beams

5. CONCLUSIONS

In this work, nonlinear finite element analyses of (RC) beams depending on two main groups were modeled and compared with a test result of an experiment done by previous researchers. The other group was modeled with variables different than the group mentioned above as a parametric study. The following inferences can be made based on the numerical findings:

1. It can be concluded that the FE model accurately predicts how the RC beams will behave. Incorporate different percentages of steel fibers (0 and 1%) and different percentages of stirrups ratio (0 and 0.335%) as well as beams that had stirrups with and without steel fibers, beside the beams with neither stirrups nor fibers.
2. The beams' length greatly impacts the beams' behaviors when the beams have a low reinforcement ratio and are strengthened with FRP at the bottom.
3. Concrete grade had an influential effect on the failure load, and it can be concluded from the percentage of increase of the failure value of concrete C33 by 16% above concrete grade C25. However, the inclusion of 1% SF had an insignificant effect on increasing the shear load carrying capacity of low-grade concrete C25 since the difference remains nearly the same percentage of 15%. A similar observation can be drawn for concrete grade C50 since the increase of failure load concrete grade C50 over C33 was 25%.
4. Using CFRP laminates at the shear zone affected of increasing the failure load by about 12% for RC beams without steel fibers.

REFERENCES

ABAQUS. Analysis of user's manual version 2014.

Abbood I., Odaa S., Hasan K., Jasim M., 2021. Properties evaluation of fiber reinforced polymers and their constituent materials used in structures – A review, *Materials Today: Proceedings*. 43, pp. 1003–1008. Doi.org/10.1016/j.matpr.2020.07.636

Abraham C., Nathan V., Jaipaul S., Nijesh D., Manoj M., Navaneeth S., 2020. Basalt fibre reinforced aluminum matrix composites–a review, Mater. *Today: Proc*., 21(1), pp. 380–383. Doi: 10.1016/J.MATPR.2019.06.135

Bloem, D.L. and Delevante, O.L., 1970. Building code requirements for reinforced concrete. ACI Journal, 1(1970), p.77.

Abbas, A., 2010. Non–linear analysis of reinforced concrete beams strengthened with steel and CFRP plates. *Diyala Journal of Engineering Sciences*, pp.249-256.

Almusallam, T.H., Elsanadedy, H.M., Al-Salloum, Y.A. and Alsayed, S.H., 2013. Experimental and numerical investigation for the flexural strengthening of RC beams using near-surface mounted steel or GFRP bars. *Construction and Building Materials*, *40*, pp.145-161. Doi:10.1016/j.conbuildmat.2012.09.107

Tiwari, A., 2019. Engineering models for shear crack width and shear deflection in slender reinforced concrete beams. Master Thesis, Delft University of Technology.

Arduini, M. and Nanni, A., 1997. Parametric study of beams with externally bonded FRP reinforcement. *Structural Journal*, *94*(5), pp.493-501. Doi:10.14359/499

Banibayat, P., 2011. Experimental investigation of the mechanical and creep rupture properties of basalt fiber reinforced polymer (BFRP) bars. Ph.D. Thesis, the University of Akron, Columbus, Ohio.

Bencardinoa, F., Rizzutia, L., and Spadea, G., 2010. Experimental evaluation of fiber reinforced concrete fracture properties. Composites Part B: Engineering, 41(1), pp. 17-24. Doi:10.1016/j.compositesb.2009.09.002

Biolzi, L., and Cattaneo, S., 2017. Response of steel fiber reinforced high strength concrete beams: experiments and code predictions, *Cement and Concrete Composites*, 77, pp. 1-13. Doi:10.1016/j.cemconcomp.2016.12.002

Chang, Y.F., Chen, Y.H., Sheu, M.S. and Yao, G.C., 2006. Residual stress–strain relationship for concrete after exposure to high temperatures. *Cement and concrete research*, *36*(10), pp.1999-2005. Doi:10.1016/j.cemconres.2006.05.029

Chellapandian M., Prakash S.S., Rajagopal A., 2017. Analytical and finite element studies on hybrid FRP strengthened RC column elements under axial and eccentric compression. *Composite Structures*, 184(15), pp. 234-248. Doi:10.1016/j.compstruct.2017.09.109

Darwin, D., Dolan, C.W. and Nilson, A.H., 2016. Design of concrete structures (Vol. 2). New York, NY, USA. McGraw-Hill Education.

Dinh, H.H., Parra-Montesinos, G.J., and Wight J.K., 2011. Shear Strength Model For Steel Fiber Reinforced Concrete Beams Without Stirrup Reinforcement. *Journal of Structural Engineering*, 137 (10), pp. 1039-1051. Doi:10.1061/(ASCE)ST.1943-541X.0000362

Hordijk, D.A., 1992. Tensile and tensile fatigue behaviour of concrete; experiments, modelling and analyses. *Heron*, *37*(1). pp. 3-79.

Hu, H.T., Lin, F.M., and Jan, Y.Y., 2004. Non-linear finite element analysis of reinforced concrete beams strengthened by fiber-reinforced plastics. *Composite Structures*, 63 (3-4), pp. 271–281. Doi:10.1016/S0263-8223(03)00174-0

Jawdhari, A. I., 2018. Finite element analysis of RC beams strengthened in flexure with CFRP rod panels, *Construction and Building Materials*, 163, pp. 751-766. Doi:10.13023/ETD.2016.113

Khalaf, M.R., Al-Ahmed, A.H.A., Allawi, A.A., El-Zohairy, A.,2021. Strengthening of continuous reinforced concrete deep beams with large openings using cfrp strips. *Materials*, 14(11), pp. 1-18. Doi:10.3390/ma14113119.

Kodur, V.K.R. and Agrawal, A., 2016. An approach for evaluating residual capacity of reinforced concrete beams exposed to fire. *Engineering Structures*, *110*, pp.293-306. Doi:10.1016/j.engstruct.2015.11.047

Li W., Huang W., Fang Y., Zhang K., Liu Z., Kong Z., 2022. Experimental and theoretical analysis on shear behavior of RC beams reinforced with GFRP stirrups, *Structures*, 46, pp. 1753-1763. Doi:10.1016/j.istruc.2022.10.138

Masmoudi, A., Ben Ouezdou, M., and Bouaziz, J., 2012. New parameter design of GFRP RC beams. *Construction and Building Materials*, 29, pp. 627-632. Doi:10.1016/j.conbuildmat.2011.11.004

Naqi, A. W., and Al-zuhairi, A. H. ,2020. Nonlinear finite element analysis of RCMD beams with large circular opening strengthened with cfrp material. *Journal of Engineering*, 26(11), pp. 170-183. Doi:10.31026/j.eng.2020.11.11

Saenz, L.P., 1964. Discussion of Equation for the Stress-Strain Curve of Concrete" by Desayi and Krishnan. *Journal of the American Concrete Institute*, *61*, pp.1229-1235.

Said, A.I. and Abbas, O.M., 2013. Serviceability behavior of high strength concrete I-beams reinforced with carbon fiber reinforced polymer bars. *Journal of Engineering*, *19*(11), pp.1515-1530. Doi: 10.31026/j.eng.2013.11.10

Said, A.I. and Tu'ma, N.H., 2021, September. Numerical modeling for flexural behavior of UHPC beams reinforced with steel and sand-coated CFRP bars. In *IOP Conference Series: Earth and Environmental Science* (Vol. 856, No. 1, p. 012003). IOP Publishing. Doi: 10.1088/1755-1315/856/1/012003

Soltani A., Harries K.A. and Shahrooz, B.M., 2013. Crack opening behavior of concrete reinforced with high strength reinforcing steel. *International Journal of Concrete Structures and Materials,* 7, pp. 253–264. Doi:10.1007/s40069-013-0054-z

Sonnenschein, R., Gajdosova, K. and Holly, I., 2016. FRP Composites and their using in the construction of Bridges. *Procedia Engineering*, *161*, pp.477-482. Doi:10.1016/j.proeng.2016.08.665.

Zana, Z.A., and Rafiq, S.K., 2019. Nonlinear finite element analysis for shear strength and behavior of reinforced concrete T-Beam with openings in both web and flange by ANSYS 14.5. *Sulaimania Journal for Engineering Sciences,* 6(4), pp. 41-50.

Zhao, J., Liang, J., Chu L., Shen, F., 2018. Experimental study on shear behavior of steel fiber reinforced concrete beams with high-strength reinforcement, *Materials MDPI*, 11(9), pp. 1-19. Doi:10.3390/ma11091682